Check for updates

Dysfunction of the heme recycling system in heme oxygenase 1–deficient mice: effects on macrophage viability and tissue iron distribution

Gennadiy Kovtunovych,[1] Michael A. Eckhaus,[2] Manik C. Ghosh,[1] Hayden Ollivierre-Wilson,[1] and Tracey A. Rouault[1]

[1]Molecular Medicine Program, Eunice Kennedy Shriver National Institute of Child Health and Human Development, Bethesda, MD; and [2]Division of Veterinary Resources, Office of Research Services, Office of the Director, National Institutes of Health, Bethesda, MD

To better understand the tissue iron overload and anemia previously reported in a human patient and mice that lack heme oxygenase-1 (HO-1), we studied iron distribution and pathology in HO-1(Hmox1)$^{-/-}$ mice. We found that resident splenic and liver macrophages were mostly absent in HO-1$^{-/-}$ mice. Erythrophagocytosis caused the death of HO-1$^{-/-}$ macrophages in in vitro experiments, supporting the hypothesis that HO-1$^{-/-}$ macrophages died of exposure to heme released on erythrophagocytosis. Rupture of HO-1$^{-/-}$ macrophages in vivo and release of nonmetabolized heme probably caused tissue inflammation. In the spleen, initial splenic enlargement progressed to red pulp fibrosis, atrophy, and functional hyposplenism in older mice, recapitulating the asplenia of an HO-1–deficient patient. We postulate that the failure of tissue macrophages to remove senescent erythrocytes led to intravascular hemolysis and increased expression of the heme and hemoglobin scavenger proteins, hemopexin and haptoglobin. Lack of macrophages expressing the haptoglobin receptor, CD163, diminished the ability of haptoglobin to neutralize circulating hemoglobin, and iron overload occurred in kidney proximal tubules, which were able to catabolize heme with HO-2. Thus, in HO-1$^{-/-}$ mammals, the reduced function and viability of erythrophagocytosing macrophages are the main causes of tissue damage and iron redistribution. (*Blood*. 2010;116(26):6054-6062)

Introduction

Humans and mice contain 2 well-characterized heme oxygenase (HO) enzymes: HO-1, which is inducible, and HO-2, which is constitutively expressed in most tissues.[1,2] HO metabolizes heme and releases free iron, carbon monoxide, and biliverdin, which quickly undergoes conversion to bilirubin. Red blood cells (RBCs) contain very high concentrations of hemoglobin (Hb),[3,4] but HO allows efficient recycling of the iron that is bound to Hb molecules in RBCs. On phagocytosis of senescent RBCs, macrophages increase their expression of HO-1 to efficiently degrade heme, and iron returns to the circulation through the iron exporter ferroportin.[5] Excess free heme is highly toxic in the circulation,[4] and protective systems exist that enable animals to avoid toxicity caused by free heme and free Hb. Hemopexin (Hpx) is a heme-binding serum protein that scavenges free heme in the circulation,[6,7] and haptoglobin (Hp) binds free Hb,[8,9] whereupon the Hb-Hp complex is endocytosed through the CD163 receptor[10] and is metabolized by macrophages.

Previous work in mouse models has shown that the lack of both HOs is embryonically lethal, whereas work on an HO-1$^{-/-}$ mouse model[11,12] and a single HO-1–deficient human patient revealed that both the HO-1$^{-/-}$ mouse and the human patient were anemic.[13] However, splenomegaly was described in the mouse model,[11,12] whereas hyposplenia was present in the human patient.[14] Hepatic and renal iron overload was observed in the patient and in mouse models, but the mechanism for iron redistribution was not clear. HO-1 deficiency was discovered in a single patient with hemolytic anemia when his physicians noted that free heme levels were elevated, but bilirubin levels were not concomitantly elevated, as would be expected in the normal response to hemolysis.[15] The patient had 2 abnormal alleles, with a complete deletion of exon 2 in the maternal allele and a 2-nucleotide deletion in exon 3 of the paternal allele.[13]

Here, to understand the redistribution of tissue iron and the anemia of the HO-1$^{-/-}$ mice and the previously described human patient, we analyzed iron parameters and macrophage populations of spleen, liver, and kidney of HO-1$^{-/-}$ mice at several ages ranging from 1.5 to 22 months, measuring expression of numerous genes, including *Hpx*, *Hp*, ferroportin (*Fpn1*, also known as *Slc40a1*), and ferritin (*Fth1*, *Ft12*). We discovered that the phenotype of HO-1$^{-/-}$ animals evolved significantly as animals aged, and the inability of erythrophagocytosing HO-1$^{-/-}$ macrophages to catabolize heme appeared to be the fundamental cause of intravascular hemolysis, tissue fibrosis, and tissue iron redistribution. Macrophages that expressed the Hp receptor CD163 were not detectable in the liver and spleens of HO-1$^{-/-}$ animals, resulting in decreased ability to clear Hb from blood. We postulate that the loss of CD163-expressing macrophages, along with the diminished ability of hepatocytes to degrade heme delivered by HPX, increased heme-dependent damage to tissues and caused a significant shift of heme uptake to the kidney.

Methods

HO-1$^{+/-}$ animals were generously donated by Anupam Agarwal and crossed as described in supplemental data (available on the *Blood* Web site;

Submitted March 1, 2010; accepted September 8, 2010. Prepublished online as *Blood* First Edition paper, September 15, 2010; DOI 10.1182/blood-2010-03-272138.

The online version of this article contains a data supplement.

The publication costs of this article were defrayed in part by page charge payment. Therefore, and solely to indicate this fact, this article is hereby marked "advertisement" in accordance with 18 USC section 1734.

© 2010 by The American Society of Hematology

Downloaded from http://ashpublications.net/blood/article-pdf/116/26/6054/1491311/zh805210006054.pdf by guest on 08 June 2024

see the Supplemental Materials link at the top of the online article) to generate HO1$^{-/-}$ animals. All animal studies were approved by the National Institute of Child Health and Human Development Animal Care and Use Committee.

Blood counts, transferrin saturation calculations, quantitative reverse-transcribed polymerase chain reaction (RT-PCR), bone marrow (BM) extraction and macrophage culture, growth of macrophage cultures, erythrophagocytosis experiments, histochemistry, and Western blots were performed as described previously,[16,17] with antibodies as described in supplemental data. Anti-HPX antibodies were a generous gift from Ann Smith (University of Missouri, Kansas City, MO).

Imaging

All images were captured in brightfield and fluorescence mode with a Nikon Eclipse E600 microscope using a Nikon DXM1200F digital camera and Nikon ACT-1 Version 2.62 software. Minimal image manipulations were performed with Adobe Photoshop Version 7.0. The following Nikon objectives were used to capture images in the indicated figure panels: 4×/0.20 (Figure 3A; original magnification, ×40), 10×/0.45 (Figure 1B left and middle panels and Figure 6B; original magnification, ×100), 20×/0.75 (Figures 5 and 6B; original magnification, ×200), 40×/1.30 oil (Figure 2C; original magnification, ×400), and 60×/1.40 oil (Figure 1B right panel; original magnification, ×600).

Results

Impact of HO-1 deficiency on spleen morphology and its functional capability: a temporal study

In comparing the previously described HO-1$^{-/-}$ mouse model[11] and a HO-1$^{-/-}$ human patient,[13] a major discrepancy between the 2 clinical descriptions was that splenomegaly was described in the HO-1$^{-/-}$ mouse, whereas the human patient had asplenia.[15] The single human patient received many different therapeutic interventions until his death at 6 years of age, and it was not clear whether the asplenia was a normal manifestation of disease or a side effect of attempted treatments.[15] To better understand the splenic pathology of HO-1$^{-/-}$ mice, we analyzed splenic function, morphology, and iron status in HO-1$^{-/-}$ mice at different ages. Spleen size was markedly increased in young HO-1$^{-/-}$ animals compared with wild-type (WT); but in older animals, the spleen size of HO-1$^{-/-}$ animals gradually diminished to smaller than WT. The spleen to brain weight ratio, a standard method of measuring organ weight changes,[18] was more than twice as high in HO-1$^{-/-}$ ($P < .001$) compared with WT mice among the animals less than 9 months old, whereas spleen size was decreased 1.6-fold ($P < .05$) in older animals compared with WT counterparts. In contrast, the spleen to brain ratios were equal in both WT age groups (Figure 1A). Histologic examination revealed that red pulp areas were enlarged in the spleens of young HO-1$^{-/-}$ mice, but red pulp areas were replaced by fibrotic tissue and fewer RBCs were observed in the shrunken spleens of older mice. This profound change in spleen morphology was readily observed on hematoxylin and eosin-stained slides from paraffin-embedded tissues (supplemental Figure 1). Masson trichrome staining revealed that significant fibrosis developed in the spleen of HO-1$^{-/-}$ animals (Figure 1B). Collagen deposition increased with age, until more than 50% of red pulp was replaced by collagen at the age of one year. Consistent with the loss of functional red pulp, large numbers of erythrocytes with Howell-Jolly bodies and numerous abnormally shaped RBCs were found on peripheral blood smears of older animals, and platelets were increased (Figure 1C). These results indicated that hyposplenia gradually develops in aging HO-1$^{-/-}$ animals during the natural course of disease, accounting for

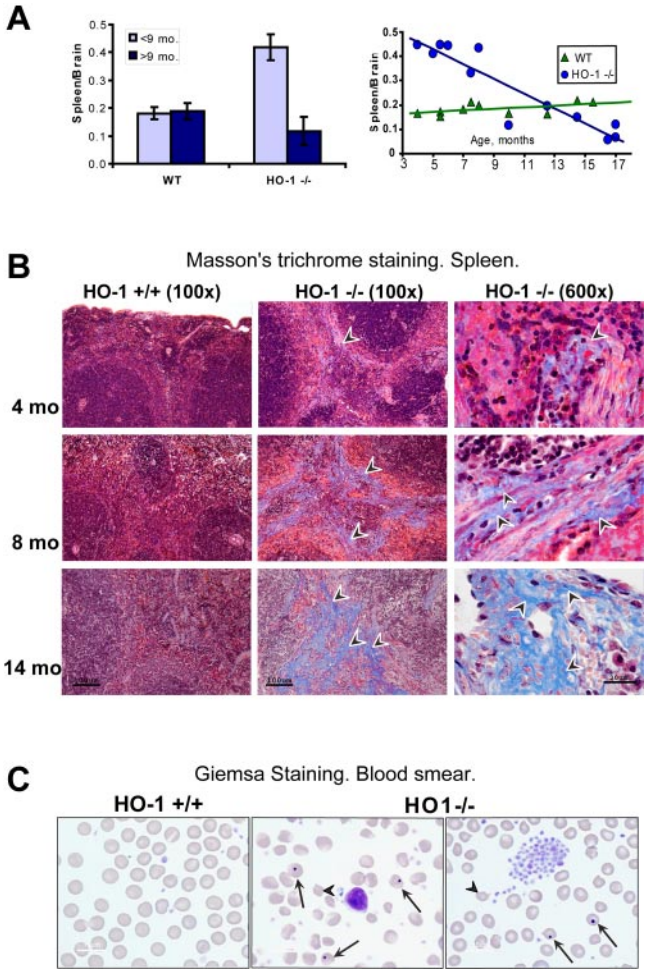

Figure 1. Splenic atrophy and fibrosis were associated with functional hyposplenism in aging HO-1$^{-/-}$ mice. (A) In mice younger than 9 months, the spleen to brain weight ratio of HO-1$^{-/-}$ mice (n = 6) was 2.3-fold ($P < .001$) higher than in WT (n = 6), whereas HO-1$^{-/-}$ mice older than 9 months (n = 6) had on average 1.6-fold ($P < .05$) smaller spleens than their WT counterparts (n = 4). Error bars represent SD of the mean. Graphing of individual spleen/brain ratios (right panel) indicated that splenic swelling was notable in young HO-1$^{-/-}$ mice, whereas older mice had progressively more severe atrophy. (B) Progressive fibrosis developed in the red pulp of aging HO-1$^{-/-}$ mice as observed by Masson trichrome histochemistry. Arrowheads point to collagen fibers, which appear as blue streaks. (C) Peripheral blood smears of HO-1$^{-/-}$ mice showed increased numbers of abnormally shaped RBCs (arrowheads) and numerous cells with Howell-Jolly bodies (arrows). Four animals from each group were examined. One typical sample of WT and 2 of HO-1$^{-/-}$ (14 months old) are shown.

abnormal peripheral blood smears and suggesting that intravascular hemolysis of senescent RBCs probably occurs. As previously reported, HO-1$^{-/-}$ mice were anemic, and transferrin saturation levels were significantly diminished (Table 1), whereas hepcidin[19] levels and erythropoietin levels were equivalent to WT levels (supplemental Figure 2). The white blood counts and neutrophils, lymphocytes, and monocytes in particular were 2-fold increased, but the differences were not statistically significant (supplemental Figure 3).

CD163^{+} macrophage depletion in spleen, liver, and BM

Expression of the Hb scavenger protein Hp was 2.2-fold increased ($P < .001$) in the liver of HO-1$^{-/-}$ mice (Figure 2A), consistent with a response to intravascular hemolysis, which probably occurred because HO-1$^{-/-}$ macrophages that phagocytosed senescent erythrocytes in the spleen and liver were prone to spontaneous rupture (Figure 3). Expression of CD163,[20] the macrophage

Downloaded from http://ashpublications.net/blood/article-pdf/116/26/6054/1491311/zh805210006054.pdf by guest on 08 June 2024

Table 1. Anemia status and transferrin iron in blood

Genotype	Hb, g/dL	HCT, %	MCV, fL	Serum iron, μg/dL	Total iron binding capacity, μg/dL	Transferrin saturation, %
HO-1$^{+/+}$	13.0 ± 0.8	47.3 ± 3.1	53.3 ± 2.9	226.1 ± 33.0	332.5 ± 43.8	67.9 ± 1.3
HO-1$^{-/-}$	10.4 ± 0.9	36.7 ± 3.0	42.0 ± 2.0	204 ± 20	513 ± 10	39.6 ± 3.3
P	.0033	.0013	.0002	.3	.0004	.0001

Data are mean ± SD.

receptor for Hb-Hp complexes, was dramatically lower in the spleen, liver, and BM of HO-1$^{-/-}$ animals (Figure 2B). Considering that CD163 expression is unique to a subset of macrophages that is incompletely defined in the mouse, this finding suggested that the size of the resident macrophage population was markedly reduced in the spleen, liver, and BM of HO-1$^{-/-}$ animals. However, CD163 expression in the HO-1$^{-/-}$ kidney (Figure 2B) was even higher than in WT, demonstrating that the presence of HO-1 was not critical for the development of CD163-expressing cells. The absence of CD163^{+} cells in the spleen, liver, and BM environment suggested that CD163^{+} macrophages could not survive in these tissues, perhaps because macrophages in these tissues have extensive contact with blood, and they consequently must contend with the high exposure to heme that results from phagocytosis of senescent RBCs and uptake of circulating Hb-Hp complexes. To use a different marker to detect tissue macrophages, we stained tissues with an antibody for the macrophage-specific marker F4/80 and again observed that the macrophage populations of spleen and liver were markedly diminished in HO-1$^{-/-}$ animals (Figure 2C). In contrast, the number of F4/80^{+} cells was higher in HO-1$^{-/-}$ kidneys, which was in good agreement with the high CD163 expression observed in HO-1$^{-/-}$ kidneys. Our data are also consistent with previous observations that HO-1$^{-/-}$ kidneys transcribe increased amounts of the monocyte attractant MCP1.[21,22]

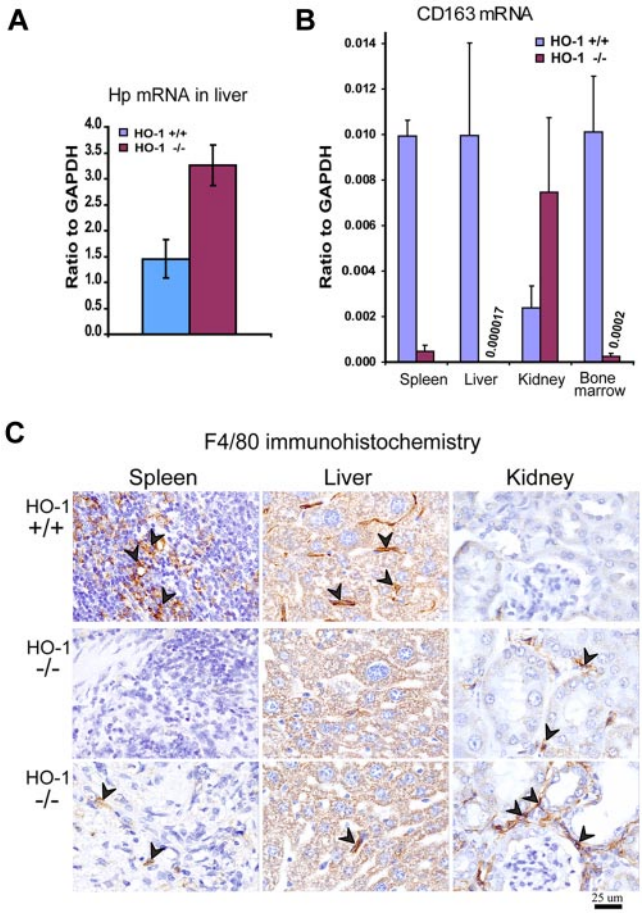

Figure 2. Macrophage depletion in tissues of HO-1$^{-/-}$ mice was associated with increased expression of Hp in the liver. (A) Quantitative RT-PCR showed 2.2-fold increased ($P < .001$) mRNA levels of Hp (Hb scavenger protein) probably in response to hemolysis of senescent RBCs. (B) Expression of the CD163, the receptor for Hb-Hp complexes, was markedly diminished in spleen, liver, and BM ($P < .001$) as determined by quantitative RT-PCR. In contrast, expression of CD163 in kidney was increased 3-fold ($P < .01$). Data were normalized to glyceraldehyde-3-phosphate dehydrogenase (GAPDH) expression (n = 5 for each WT and HO-1$^{-/-}$ mice). All mice were 12 months old. Error bars represent SD of the mean. (C) Immunohistochemistry for the pan-macrophage marker, F4/80, indicated that the resident macrophage populations of the spleen and liver were markedly reduced in HO-1$^{-/-}$ animals. Arrowheads point to diaminobenzidine positively stained macrophages (brown staining). The increased number of F4/80^{+} cells in kidneys correlates with the elevated CD163 expression. Two different fields are shown for the tissue samples of the same HO-1$^{-/-}$ mice. All animals were 12 months old.

Progressive death of erythrophagocytosing HO-1–deficient BMDMs

To test the hypothesis that erythrophagocytosis (EPC) can be damaging for HO-1–deficient macrophages, we cultured BM-derived macrophages (BMDMs) from WT and HO-1$^{-/-}$ animals and exposed the macrophages to RBCs opsonized with antimouse RBC antibodies in vitro. The differentiation, proliferation rate, and morphologic characteristics of macrophages from HO-1$^{-/-}$ animals were indistinguishable from their WT counterparts, and the ability of macrophages to phagocytose pretreated erythrocytes was equally efficient in HO-1$^{-/-}$ and WT macrophages (Figure 3A). Indeed, each cell was able to phagocytose all of the RBCs with which it made physical contact, engulfing from one to 20 erythrocytes simultaneously. The difference between WT and HO-1$^{-/-}$ macrophages started to develop 3 to 5 hours after phagocytosis when active processes of digestion took place. We observed partial restoration of cell morphology in some WT cells 3 to 5 hours after phagocytosis, and WT cells developed normal spreading and attachments by 24 hours, whereas the morphology of HO-1$^{-/-}$ cells was distinctly abnormal at 24 hours: cell bodies remained shrunken and did not regain their normal shape (Figure 3A).

To investigate the integrity of HO-1$^{-/-}$ macrophages after EPC, we used a lactate dehydrogenase (LDH)-based toxicology assay. Four hours after EPC, 13% of total LDH was detected in the culture medium of both WT and HO-1$^{-/-}$ BMDMs. The fraction of LDH found in the culture media of WT cells increased only slightly to 17% and 18% at time points 17 and 24 hours, respectively (Figure 3B). In contrast, HO-1$^{-/-}$ cells released 51% and 59% of LDH 17 and 24 hours after EPC, which corresponded to 3- and 3.3-fold increases, respectively ($P < .001$) compared with the WT cells (Figure 3B). After EPC, HO-1 mRNA expression rose sharply in WT BMDMs, increasing 5-, 37-, and 33-fold at the 1, 3, and 6-hour time points, respectively, compared with control, and later quickly returning to near the baseline level, consistent with the importance of this gene in maintaining safe levels of heme within cells. As HO-2 expression is not inducible, HO activity did not increase after EPC, even in the HO-1$^{-/-}$ cells (Figure 3C bottom panel), and lack

Downloaded from http://ashpublications.net/blood/article-pdf/116/26/6054/1491311/zh805210006054.pdf by guest on 08 June 2024

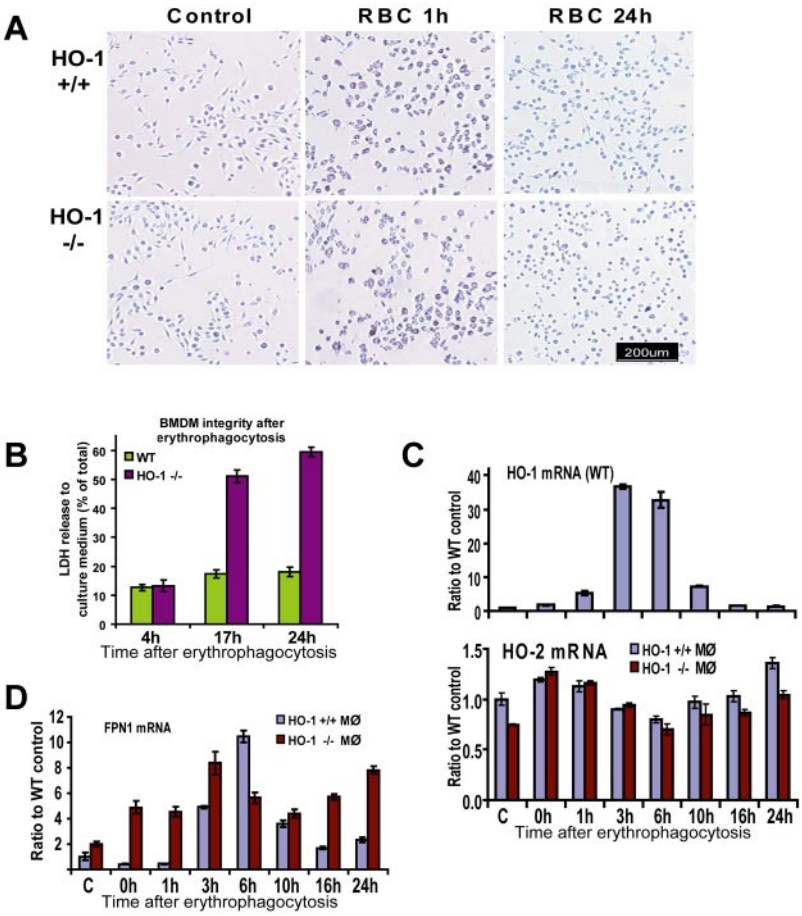

Figure 3. BMDMs of HO-1$^{-/-}$ mice did not survive EPC in vitro. (A) Bright-field pictures taken before and 1 hour after EPC showed no apparent difference between HO-1$^{-/-}$ and HO-1$^{+/+}$ BMDMs. However, after 24 hours, WT macrophages returned to their normal pretreatment appearance, whereas HO-1$^{-/-}$ macrophages were shrunken and did not regain their normal shape. (B) Measurements of cytosolic enzyme LDH in the culture medium showed that cells were equally intact in WT and HO-1$^{-/-}$ samples 4 hours after EPC with the release of 12% of activity to the medium. At the 17- and 24-hour time points, LDH levels in the medium of HO-1$^{-/-}$ cells were 51% and 59%, correspondingly 3- and 3.3-fold ($P < .001$) higher compared with WT. Error bars represent SD of the mean. (C) Quantitative RT-PCR demonstrated that HO-1 levels increased 5-, 37-, and 33-fold ($P < .001$) in WT cells 1, 3, and 6 hours after EPC, respectively (values are shown as ratios to actin-β). HO-1 expression returned to near the baseline levels 16 and 24 hours after treatment in WT cells. HO-2 levels did not increase in HO-1$^{-/-}$ cells after EPC. (D) In WT FPN1, mRNA levels increased 11-fold 6 hours after EPC and subsequently decreased, showing a similar pattern to the HO-1 mRNA levels. This pattern of expression was distorted in HO-1$^{-/-}$ BMDMs, with FPN1 levels 11-, 10-, 3-, and 3-fold higher at the 0-, 1-, 16-, and 24-hour time points, respectively ($P < .001$), than in WT cells. Different mice were used for different independent experiments where similar results were obtained. For each particular experiment, BM from either one WT or one HO-1$^{-/-}$ mouse (age- and sex-matched) was used as a source of BMDMs.

of sufficient HO probably caused significant stress mediated by free heme. When iron was released as a result of heme breakdown by HO-1 in WT macrophages, mRNA expression levels of the iron exporter Fpn1 increased. We observed that expression of Fpn1 correlated with HO-1 expression in WT macrophages, suggesting its importance in exporting iron released from heme (Figure 3D). In WT, Fpn1 mRNA levels increased up to 10-fold at 3 and 6 hours after EPC, and subsequently decreased. In contrast, this pattern of expression was distorted in HO-1–deficient microphages. The main differences from WT consisted of higher Fpn1 expression in HO-1$^{-/-}$ at the 0-, 1-, 16-, and 24-hour time points (11-, 10-, 3-, and 3-fold; $P < .001$) compared with Fpn1 levels in WT (Figure 3D). This chronic elevation of Fpn1 mRNA expression in HO-1$^{-/-}$ cells may be explained by the fact that the enhancer region of Fpn1 contains an active MARE/ARE element, which is inducible by heme and is the binding site for the transcriptional repressor Bach1 or the positive regulator Nrf2.[23] When heme binds to Bach1, its repressor activity is attenuated and Bach1 undergoes degradation in the cytosol. As a pro-oxidant, heme is involved in a process that stabilizes the positive regulator Nrf2.[23] Both Hmox1 and Fpn1 contain a MARE/ARE regulatory element in their upstream regulatory region, which may explain their coordinated expression in WT macrophages in response to heme challenge (Figure 3C-D).

Increased HPX expression in liver, and its depletion in serum of HO-1$^{-/-}$ mice

Hpx is the major inducible heme-binding protein in serum.[6] Both mRNA and protein levels of Hpx were significantly increased in liver lysates of HO-1$^{-/-}$ mice (Figure 4A-B). mRNA levels were increased 5-fold in mice older than 12 months (Figure 4A) and 1.7-fold in 4- to 8-month-old mice ($P < .05$). Even at the age of 7 weeks, Hpx protein and mRNA levels were slightly increased, although results were not statistically significant (not shown). Although the liver is the major site of Hpx expression, Hpx mRNA levels were also detectable in kidney and spleen. The trends and magnitude of Hpx mRNA changes in kidney and spleen (not shown) were, on average, very similar to those in liver. The increase of Hpx protein expression levels in the HO-1$^{-/-}$ kidney was even more pronounced than in liver (Figure 4B-C), although the absolute quantity of kidney Hpx was much lower in kidney lysates. The apparent increase of Hpx protein in the HO-1$^{-/-}$ sample in kidney (Figure 4C) compared with Hpx in liver (Figure 4B) occurred because a longer film exposure was necessary to visualize Hpx in the WT kidney lysates. The simultaneous induction of Hpx expression in several different tissues suggests that Hpx expression may be induced by heme-mediated inflammatory stimuli. In a Western blot analysis of serum, we found that serum Hpx levels were lower in the HO-1$^{-/-}$ than in WT mice (Figure 4D). This contradiction between increased hepatic expression and reduced serum levels was previously observed after experimental injection of hemin, 35 or 70 μg/kg, in WT mice.[24] An even more severe decrease in serum Hpx level was reported in an HO-1–deficient patient who had undetectable levels of Hpx in serum and died at the age of 6 years.[13] It is reasonable to postulate that Hpx is consumed at a much higher pace in HO-1$^{-/-}$ mice because it scavenges free circulating heme. Hpx binds free heme and the heme-Hpx complexes are taken up by the receptor LRP1/CD91 in

Downloaded from http://ashpublications.net/blood/article-pdf/116/26/6054/1491311/zh805210006054.pdf by guest on 08 June 2024

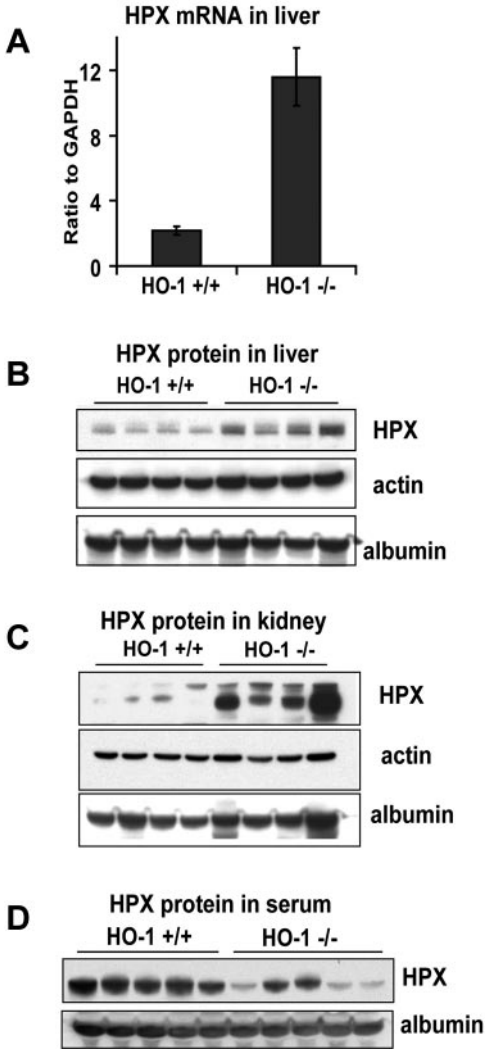

Figure 4. Hpx expression and consumption increased in HO-1$^{-/-}$ mice. (A) mRNA expression of HPX was 5-fold higher ($P < .001$) in HO-1$^{-/-}$ liver as measured by quantitative RT-PCR. Error bars represent SD of the mean. Western blot analyses of liver (B) and kidney (C) lysates showed higher levels of HPX protein in HO-1$^{-/-}$ animals in these organs. Actin blots represent tissue protein loading controls. Albumin blots were used to indicate the level of blood contamination in the tissue. (D) Serum levels of Hpx in HO-1$^{-/-}$ mice were on average lower than those of WT, consistent with intense usage of HPX for heme clearance and pointing to incomplete recycling of HPX. Serum was diluted for loading, and an equivalent of 0.5 μL of serum was loaded in each lane. (A-D) Mice were 8 months old, on average. Each panel represents one of 3 independent experiments performed on different groups of mice.

several different types of cells, including macrophages, hepatocytes, neurons, and syncytiotrophoblasts.[25] Under physiologically normal conditions, heme-Hpx complexes that attach to the Lrp1 receptor on the surface of hepatocytes are internalized through endocytosis, heme is released in the acidic environment of endosomes, and Hpx is thought to be released intact into the bloodstream.[26-28] However, under conditions of hemolysis, when large amounts of heme are released into circulation, saturation of the recycling system may occur, and it is thought that significant amounts of heme-Hpx complexes can be processed in lysosomes, which leads to degradation and depletion of serum Hpx.[25] The endothelial injuries that were observed in HO-1$^{-/-}$ mice may allow penetration of heme-Hpx as well as heme-albumin complexes into the glomerular filtrate, and reabsorption may occur in the proximal tubule through nonspecific uptake mechanisms that involve megalin and cubulin receptor-mediated uptake.[29,30] This notion is partially supported by results displayed in Figure 4C, where markedly increased levels of Hpx were observed in the lysates of HO-1$^{-/-}$ kidneys.

Iron redistribution in spleen, kidney, and liver tissues of HO-1$^{-/-}$ mice

To comprehensively analyze changes in tissue iron distribution in HO-1$^{-/-}$ mice, we performed Perls Prussian blue staining on paraffin-embedded tissues. We observed that iron staining was markedly diminished in spleens of HO-1$^{-/-}$ mice regardless of the age of the mouse (Figure 5A). Because most iron in WT spleens resides in macrophages, which are responsible for recycling iron from Hb of senescent RBCs, the lack of splenic HO-1$^{-/-}$ macrophages probably accounts for reduced spleen iron.

In the kidney, we observed a distinct pattern of increased iron staining in epithelial cells of the proximal tubules and some glomeruli (Figure 5A), similar to previous observations.[21] The phenomenon of significant iron increase in kidney is usually associated with diseases that increase intravascular hemolysis, such as sickle cell disease, malaria, and artificially induced intravascular hemolysis. The rerouting of iron to the kidney generally occurs when the heme-Hpx or Hb-Hp scavenging systems are compromised. For instance, in Hp null mice, Hb from lysed erythrocytes cannot be catabolized by CD163-expressing macrophages, and Hb is consequently trapped in the kidney where heme iron is extracted and deposited in proximal tubules. Similar proximal tubular iron overload is observed when intravascular hemolysis occurs in Hpx

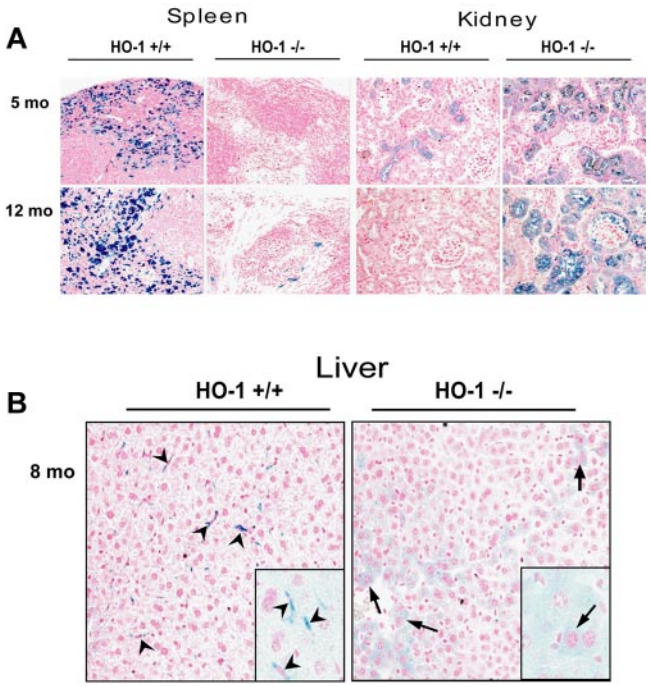

Figure 5. Redistribution of iron from splenic and hepatic macrophages to hepatocytes and renal proximal tubule cells in HO-1$^{-/-}$ mice. (A) Perls Prussian blue staining of paraffin-embedded tissue sections revealed pronounced high iron levels in splenic macrophages of the WT, compared with almost undetectable macrophage iron in the HO-1$^{-/-}$ animals, whereas very little iron was detected in renal proximal tubules of the WT, but iron levels were greatly increased in the renal proximal tubules of HO-1$^{-/-}$ mice. Slices of paraffin-embedded tissue from 2 mice (5 and 12 months old) for both WT and HO-1$^{-/-}$ are shown. (B) Redistribution of iron in liver from Kupffer cells (arrowheads), which were absent in HO-1$^{-/-}$ mice, to hepatocytes (arrows). (Inset) A 2.5-fold digital magnification of an area from the adjacent field, to better demonstrate the different morphologies of iron-containing cells in WT versus HO-1$^{-/-}$ animals.

Downloaded from http://ashpublications.net/blood/article-pdf/116/26/6054/1491311/zh805210006054.pdf by guest on 08 June 2024

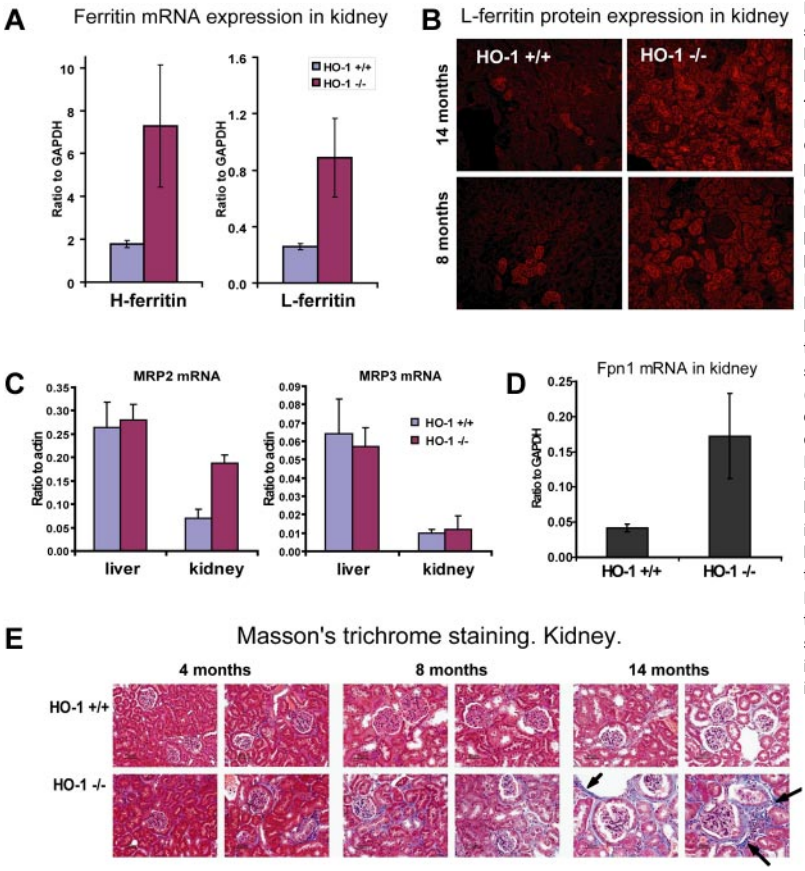

Figure 6. Increased L- and H-ferritin, FPN1, and MRP2 expression and fibrosis in HO-1$^{-/-}$ kidneys reflected the shift of heme-iron recycling. (A) Both L and H ferritin mRNA expression levels were increased in kidney of HO-1$^{-/-}$ mice. L ferritin increased 4.1-fold ($P < .01$) and H ferritin increased 3.5-fold ($P < .01$) as revealed by quantitative RT-PCR. Animals 8 months of age (n = 4 in each group) were used to generate data that are represented in panels A, C, and D. Error bars represent SD of the mean. (B) Immunofluorescence analysis for L-ferritin indicated that protein levels were also increased in the HO-1$^{-/-}$ kidney. Most ferritin protein was found in proximal tubules and in some glomeruli. This pattern replicated the iron localization pattern revealed by the Perls Prussian blue staining and suggested that most accumulated iron in kidney was stored in the form of ferritin. (C-D) mRNA expression levels of MRP2, MRP3 normalized to actin-β, and FPN1 normalized to glyceraldehyde-3-phosphate dehydrogenase (GAPDH) expression were obtained by quantitative RT-PCR. (C) A 2.7-fold increase ($P < .001$) in expression of the apical membrane exporter of conjugated bilirubin, MRP2, in HO-1$^{-/-}$ kidney suggested that heme degradation occurred in the polarized cells of the proximal tubules. Levels of MRP3, a widely expressed bilirubin exporter of nonpolarized cells, including macrophages, remained unchanged. mRNA levels of MRP2 and MRP3 remained unchanged in liver. (D) A 4-fold increase ($P < .01$) in FPN1 mRNA expression was observed in kidney, which probably served to return iron from catabolized heme to the circulation. (E) Fibrotic damage occurred to the kidney of HO-1$^{-/-}$ mice as a result of heme iron recycling, as seen on Masson trichrome–stained paraffin-embedded tissue sections, where fibrosis developed in aging HO-1$^{-/-}$ mice at much higher levels than in WT animals. Arrows indicate collagen fibers, which are colored in blue.

null mice.[8] Increased numbers of macrophages were observed with intensely positive iron staining in the interstitial areas between proximal tubules of HO-1$^{-/-}$ mice (Figure 2C). Although macrophages are in intimate contact with renal tubules from early in development,[31] renal macrophages are not thought to have an important role in phagocytosis of circulating senescent RBCs, which may account for the prolonged survival of macrophages in the kidney relative to the spleen and liver. The macrophages we observed in kidney were probably inflammatory macrophages attracted by signaling molecules, including perhaps MCP1,[32] released by kidneys that were damaged by exposure to Hb and free heme and had decreased ability to process heme. Thus, these macrophages probably participate in removal of damaged cells from some injured proximal tubules, and these macrophages may acquire their increased iron through phagocytosis of damaged renal cells.

Increased iron deposition in the liver of HO-1$^{-/-}$ mice has been previously reported,[11] and we also found increased liver iron (Figure 5B), although changes were not as striking as those we observed in spleen and kidney (Figure 5A). Hepatocytes had increased iron staining in HO-1$^{-/-}$ mice, perhaps because hepatocytes of HO-1$^{-/-}$ mice had to process increased amounts of heme-Hpx complexes, leading to increased hepatocytic iron stores.[33] In contrast to the increased iron in hepatocytes, almost no iron-positive Kupffer cells were present in HO-1$^{-/-}$ liver, whereas Kupffer cells were loaded with iron in WT livers (Figure 5B). Thus, the main difference between WT and HO-1$^{-/-}$ liver appeared to reflect a redistribution of iron between different liver cell types, rather than a significant overall increase in tissue iron content. Indeed, preliminary measurements of total nonheme iron showed no significant difference between WT and HO-1$^{-/-}$ liver iron levels (not shown). The iron staining results were entirely consistent with our finding that lower numbers of macrophages were present in the spleens and livers of HO-1$^{-/-}$ animals.

Heme iron recycling in HO-1$^{-/-}$ kidney

To understand the significance and fate of the iron overload in the proximal tubules of HO-1$^{-/-}$ mice, we assessed expression of key iron transport and storage proteins, including FPN1, H and L ferritin, and the putative bilirubin exporters, multidrug resistance-associated proteins 2 (Mrp2) and 3 (Mrp3) in kidney lysates. Our results suggested that heme is metabolized by HO-2, which is constitutively expressed in most tissues at modest levels. Extra iron released from heme can be either stored in ferritin within proximal tubule cells or exported into the circulation by FPN1. H and L ferritin mRNA levels were significantly increased in HO-1$^{-/-}$ kidney as measured by quantitative RT-PCR (Figure 6A). Increased L ferritin expression was observed in proximal tubules by immunofluorescence assays (Figure 6B). We also performed Western analysis of H and L ferritin in kidney lysates (not shown), and the results were consistent with quantitative RT-PCR data. Despite its lack of HO-1, the kidney appears to partially substitute for the spleen as a buffer for heme iron exchange. We also found that FPN1 mRNA expression increased 4-fold ($P < .01$) in kidneys of HO-1$^{-/-}$ mice (Figure 6D). The increased FPN1 expression in HO-1$^{-/-}$ kidneys probably increased their capacity to return iron to the circulation, and supports the idea that the kidneys can recycle iron retrieved from heme in the glomerular filtrate.

To support the idea that heme catabolism in kidney is substantially higher in HO-1$^{-/-}$ mice, we analyzed expression levels of Mrp2 and Mrp3. These proteins are thought to function as

Downloaded from http://ashpublications.net/blood/article-pdf/116/26/6054/1491311/zh805210006054.pdf by guest on 08 June 2024

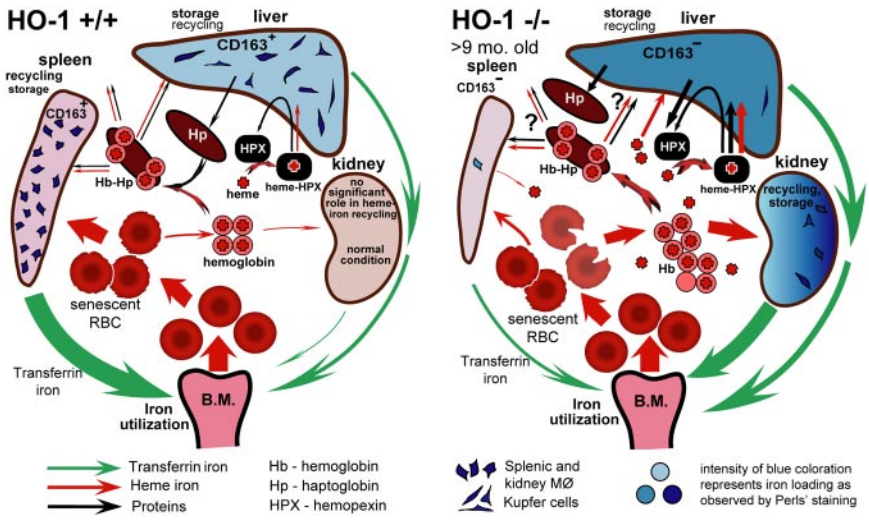

Figure 7. Model of heme-iron recycling and tissue iron redistribution in HO-1$^{-/-}$ mice. Splenic macrophages that phagocytose senescent RBCs die in HO-1$^{-/-}$ mice. The contents released from dying macrophages include nonmetabolized heme, which damages surrounding cells and causes fibrosis in red pulp areas of the spleen, thereby eliminating the normal setting in which recycling of RBCs usually occurs. Senescent RBCs rupture in the circulation, releasing Hb and heme. The liver increases synthesis of Hp and Hpx, but there are few viable macrophages remaining in the spleen and liver that can recycle Hb-Hp complexes through the CD163 receptor. Iron stores shift from liver and splenic macrophages to hepatocytes and kidney proximal tubules where Hb and, perhaps, other heme moieties are reabsorbed, and iron can be recovered from heme by HO-2 enzymatic activity. The intensity of blue coloration represents iron loading as observed by Perls Prussian blue staining. Red and green arrows represent directions of heme and transferrin iron flows, respectively. Black arrows represent flow of proteins, such as Hp and Hpx. The thickness of each particular arrow reflects the proportional flux of transferrin iron, heme iron, and other important molecules, such as Hpx and Hp, as proposed by the model. The difference in spleen size shown in the figure is relevant for HO-1$^{-/-}$ mice at the age of 9 months and older.

transmembrane exporters for bilirubin, a product of heme catabolism. The mRNA expression levels of Mrp2 were 3-fold increased in the kidney but were unchanged in the liver of HO-1$^{-/-}$ mice (Figure 6C), whereas the ubiquitously expressed bilirubin exporter of nonpolarized cells, Mrp3, was unchanged in both liver and kidney. Mrp2 is known to localize to the apical membrane of polarized cells, such as the canalicular membrane of hepatocytes, kidney proximal tubule epithelial cells, and enterocytes of the small intestine.[34] It is very probable that Mrp2 expression is elevated in the HO-1$^{-/-}$ kidneys to secrete the extra bilirubin that they generate from increased heme catabolism.

Although normal blood urea nitrogen and creatinine levels suggested that renal function was not significantly compromised, we observed evidence of renal damage in older animals. Masson trichrome staining revealed higher levels of collagen deposition in the kidneys of HO-1$^{-/-}$ than in WT mice. Increased collagen deposition was especially pronounced in 14-month-old mice (Figure 6E) consistent with previous observations.[21] Development of fibrosis suggested that the kidneys of HO-1$^{-/-}$ mice were exposed to a pathologic challenge, which probably consisted mainly of increased levels of heme in blood and glomerular filtrate.

Discussion

Heme is a unique compound that serves as a cofactor in proteins involved in oxygen transport, respiration, regulation of gene expression, and numerous enzymatic activities.[3,4] However, excess heme can be very toxic, and intracellular heme biosynthesis is tightly regulated and coordinated with synthesis of heme-containing proteins. Constitutive expression of HO-2 is sufficient to protect most cells from heme toxicity and to provide antioxidant protection by supplying cells with carbon monoxide, biliverdin, and bilirubin. However, HO-2 is not inducible, and it cannot fully catabolize large amounts of heme that are delivered from external sources such as erythrocytes. Expression of inducible HO-1 allows cells to quickly increase the HO activity to maintain safe levels of heme within cells. In the present study of the HO-1$^{-/-}$ mouse, we attempted to understand the mechanism that underlies the major phenotypic developments in HO-1–deficient mammals. The findings summarized in our proposed model (Figure 7) suggest that disruption of normal recycling of erythrocytes by splenic and liver macrophages is, perhaps, the main factor that leads to other developments, including hyposplenism, intravascular hemolysis, endothelial and liver injury, and iron redistribution. It is also possible that depletion of macrophages in the BM contributed to the anemia.

Phagocytosis of senescent RBCs occurs mainly in the splenic macrophages and hepatic Kupffer cells. We observed that macrophages were almost completely absent in the spleen and liver of HO-1$^{-/-}$ mice, as revealed both by extremely low expression of CD163, a macrophage-specific receptor for Hp-Hb complexes, and loss of the F4/80 immunohistochemical signal for macrophages (Figure 2B-C). We postulated that splenic macrophages died because they could not efficiently metabolize the heme contained in phagocytosed RBCs, analogous to the cell death that has been observed in normal macrophages that ingest too many RBCs,[35] and that absence of splenic macrophages accounted for the observed splenic iron depletion (Figure 5A). In HO-1$^{-/-}$ mice, macrophages were also markedly reduced in the BM, as assessed by CD163 mRNA determinations, but CD163 expression was increased in the kidneys (Figure 2B) of HO-1$^{-/-}$ mice, suggesting that there are no intrinsic problems with maturation of CD163 macrophages in HO-1$^{-/-}$ animals. We demonstrated that EPC has a very adverse effect on HO-1$^{-/-}$ macrophages in in vitro experiments. BMDMs from HO-1$^{-/-}$ mice successfully phagocytosed RBCs, but they could not recover from heme stress, in contrast to WT BMDMs (Figure 3A), and they lost their cellular integrity and released the cytosolic enzyme LDH into the culture medium 24 hours after EPC (Figure 3B). Kidney tissue macrophages may survive (Figure 2B-C) because they have no direct contact with blood, whereas splenic, hepatic, and BM erythrophagocytosing macrophages develop heme overload through EPC and increased Hb-Hp uptake. We suggest that there is a constant flow of monocytes into tissues, as we found that the number of monocytes in peripheral blood was not decreased in the HO-1$^{-/-}$ animals (supplemental Figure 3), and numerous F4/80^{+} cells were observed within some vascular infiltrates in large liver vessels of HO-1$^{-/-}$ mice (supplemental Figure 4B).

In HO-1$^{-/-}$ animals, senescent RBCs were no longer efficiently removed from the circulation, which probably led to increased intravascular hemolysis and a concomitant increase in levels of

Downloaded from http://ashpublications.net/blood/article-pdf/116/26/6054/1491311/zh805210006054.pdf by guest on 08 June 2024

circulating Hb and heme. Hepatocytes responded to hemolysis by markedly increasing synthesis of the heme-scavenger protein Hpx (Figure 4) and the Hb-scavenger protein Hp (Figure 2A). Heme-Hpx complexes are mostly cleared in liver, which can explain the increased iron levels observed in hepatocytes (Figure 5B). Inefficiency of heme catabolism in the absence of HO-1 has been previously reported to cause hepatic injury.[12] The observed depletion of Hpx in the serum of HO-1$^{-/-}$ mice implies that Hpx and its recycling system have been intensively used to the point of saturation. Hb-Hp complexes are usually taken up by splenic and liver CD163^{+} macrophages. Profound deficiency of these cells necessarily results in inefficient uptake of Hb-Hp complexes in the liver and spleen. As alternative mechanisms for removal of Hb-Hp from the circulation are unknown, the fate of these Hb-Hp complexes remains to be clarified. It is also unclear whether heme delivered to macrophages in Hb-Hp complexes through the CD163 receptor causes as much harm to the cells as does Hb that is obtained through EPC.

We propose that renal iron overload arises from uptake of Hb and other heme-binding proteins by proximal tubule cells after the macrophage-mediated heme recycling system is damaged. Increased expression of H and L ferritin in the proximal tubule cells, increased expression of the bilirubin exporter specific to polarized cells, Mrp2, and high renal expression of Fpn1 (Figure 6A-D) all lead to the supposition that heme is successfully catabolized by the kidney, with release of iron through Fpn1 and bilirubin through Mrp2. Export of bilirubin directly into the urine represents an efficient way for an organism to rid itself of bilirubin when hemolysis occurs. Proximal tubule cells can metabolize heme using HO-2, and we postulate that they are spared the immediate toxic death observed in macrophages because they are exposed to the lower levels of heme in glomerular filtrate, rather than to the bolus of heme released when RBCs are phagocytosed.

Our work demonstrates several previously unknown points about HO-1$^{-/-}$ mice that may be important in the correct diagnosis of human counterparts. In the natural history of the disease, splenomegaly develops initially, but hyposplenism develops in older HO-1$^{-/-}$ mice and is associated with complete loss of splenic macrophages and red pulp atrophy. Fibrosis develops in HO-1$^{-/-}$ spleens, and splenic size gradually diminishes as scarring progresses. The peripheral blood smear shows typical elements associated with hyposplenism, including RBCs with Howell-Jolly bodies. The anemia of HO-1$^{-/-}$ may be partly caused by inflammation[4] and partly attributable to the functional iron deficiency that was revealed by the decreased transferrin saturations of the HO-1$^{-/-}$ compared with WT littermates of the same background that we reported here. We did not further analyze systemic inflammation in this study, but we observed lymphocytic infiltrates and rarely some F4/80^{+} macrophages in blood vessel walls (supplemental Figure 4). Because inflammation generally increases hepcidin expression, whereas iron deficiency diminishes hepcidin expression, we suggest that hepcidin levels did not change (supplemental Figure 2) because these 2 opposing forces simultaneously influenced hepcidin expression. As outlined in Figure 7, we suggest that the loss of hepatic and splenic macrophages shifts heme degradation to renal proximal tubules, which leads to renal fibrosis in older animals, and that splenic iron levels are low because of the loss of macrophages. In the liver, where Kupffer cells are almost undetectable, hepatocytic iron levels increase, probably because of uptake of large amounts of heme from heme-HPX complexes. Increased circulating heme and Hb leads to iron overload in renal proximal tubules.

Our demonstration that HO-1$^{-/-}$ macrophages may die on EPC and that most of the pathologic changes of the spleen, liver, and kidney result from necrosis of macrophages suggests that patients with HO-1$^{-/-}$ deficiency could possibly be cured by BM transplantation. Normal macrophage progenitor cells could potentially restore populations of splenic and liver macrophages, which would lead to restoration of the RBC and heme recycling system. Restoration of this system would diminish hemolysis and restore Hb-Hp clearance, which would minimize the damage caused by free heme to other tissues. The anemia would also probably be cured because normal iron recycling by macrophages would be restored and inflammatory stimuli would be minimized.

It is important to address the issue of relevance of our findings to human patients. There is apparently a difference between the ability of humans and mice to survive lack of HO-1 activity, as the reported human phenotype appeared to be more severe than we observed in the HO-1–deficient mice on mixed C57BL/6-FVB background. The possible cause of enhanced mouse survival may depend on a difference in biochemistry of the species. The mouse can synthesize large amounts of ascorbic acid, which helps to prevent oxidation of extracellular Hb to met-Hb. In contrast, humans cannot produce ascorbic acid; and by analogy with other species, it is probable that humans are prone to a much higher rate of heme oxidation than mice.[36] Oxidized heme more readily dissociates from the Hb molecule, and free heme is more harmful than bound heme. Thus, it is possible that complete absence of HO-1 in humans is not compatible with survival.

Nevertheless, we think there is much in common between the mouse and human HO-1$^{-/-}$ phenotypes, including anemia, hyposplenism, endothelial, liver, and kidney injuries, and serum HPX depletion. The accumulation of Hp, which was reported in an HO-1–deficient patient,[15,37] suggests that the patient most probably had fewer CD163-expressing macrophages because the serum Hp would have otherwise been depleted by the severe hemolysis observed in the patient. Thus, on the assumption that mechanisms of developing pathology at HO-1 deficiency are similar in both organisms, approaches developed for treatment of mice can be useful for therapy of HO-1–deficient patients. The hypothesis that BM transplantation would cure HO-1$^{-/-}$ animals can be readily tested in HO-1$^{-/-}$ mice and considered as a treatment for human HO-1–deficient patients. We anticipate that patients with partial loss of HO-1 function may exist and have less severe symptoms than were described for the reported human patient, and we suggest that our findings can help to identify other human HO-1–deficient patients.

Acknowledgments

The authors thank Stefania Pittaluga and Ann Smith for productive discussions and advice.

This work was supported by the National Institute of Child Health and Human Development (intramural program).

Authorship

Contribution: G.K. designed research, performed most experiments, analyzed data, and wrote the paper; M.A.E. and M.C.G. performed experiments and analyzed data; H.O.W. performed

Downloaded from http://ashpublications.net/blood/article-pdf/116/26/6054/1491311/zh805210006054.pdf by guest on 08 June 2024

experiments; and T.A.R. oversaw the study, designed research, analyzed data, and wrote the paper.

Conflict-of-interest disclosure: The authors declare no competing financial interests.

Correspondence: Tracey A. Rouault, Eunice Kennedy Shriver National Institute of Child Health and Human Development, 9000 Rockville Pike, Bldg 18T, Rm 101, Bethesda, MD 20892; e-mail: trou@helix.nih.gov.

References

1. Tracz MJ, Alam J, Nath KA. Physiology and pathophysiology of heme: implications for kidney disease. *J Am Soc Nephrol.* 2007;18(2):414-420.
2. Balla J, Vercellotti GM, Jeney V, et al. Heme, heme oxygenase, and ferritin: how the vascular endothelium survives (and dies) in an iron-rich environment. *Antioxid Redox Signal.* 2007;9(12):2119-2137.
3. Schechter AN. Hemoglobin research and the origins of molecular medicine. *Blood.* 2008;112(10):3927-3938.
4. Belcher JD, Beckman JD, Balla G, Balla J, Vercellotti G. Heme degradation and vascular injury. *Antioxid Redox Signal.* 2010;12(2):233-248.
5. Zhang AS, Enns CA. Molecular mechanisms of normal iron homeostasis. *Hematology Am Soc Hematol Educ Program.* 2009:207-214.
6. Tolosano E, Altruda F. Hemopexin: structure, function, and regulation. *DNA Cell Biol.* 2002;21(4):297-306.
7. Morgan WT, Muster P, Tatum F, Kao SM, Alam J, Smith A. Identification of the histidine residues of hemopexin that coordinate with heme-iron and of a receptor-binding region. *J Biol Chem.* 1993;268(9):6256-6262.
8. Fagoonee S, Gburek J, Hirsch E, et al. Plasma protein haptoglobin modulates renal iron loading. *Am J Pathol.* 2005;166(4):973-983.
9. Kato GJ. Haptoglobin halts hemoglobin's havoc. *J Clin Invest.* 2009;119(8):2140-2142.
10. Moestrup SK, Moller HJ. CD163: a regulated hemoglobin scavenger receptor with a role in the anti-inflammatory response. *Ann Med.* 2004;36(5):347-354.
11. Poss KD, Tonegawa S. Heme oxygenase 1 is required for mammalian iron reutilization. *Proc Natl Acad Sci U S A.* 1997;94(20):10919-10924.
12. Poss KD, Tonegawa S. Reduced stress defense in heme oxygenase 1-deficient cells. *Proc Natl Acad Sci U S A.* 1997;94(20):10925-10930.
13. Yachie A, Niida Y, Wada T, et al. Oxidative stress causes enhanced endothelial cell injury in human heme oxygenase-1 deficiency. *J Clin Invest.* 1999;103(1):129-135.
14. Kawashima A, Oda Y, Yachie A, Koizumi S, Nakanishi I. Heme oxygenase-1 deficiency: the first autopsy case. *Hum Pathol.* 2002;33(1):125-130.
15. Koizumi S. Human heme oxygenase-1 deficiency: a lesson on serendipity in the discovery of the novel disease. *Pediatr Int.* 2007;49(2):125-132.
16. Meyron-Holtz EG, Ghosh MC, Rouault TA. Mammalian tissue oxygen levels modulate iron-regulatory protein activities in vivo. *Science.* 2004;306(5704):2087-2090.
17. LaVaute T, Smith S, Cooperman S, et al. Targeted deletion of the gene encoding iron regulatory protein-2 causes misregulation of iron metabolism and neurodegenerative disease in mice. *Nat Genet.* 2001;27(2):209-214.
18. Michael B, Yano B, Sellers RS, et al. Evaluation of organ weights for rodent and nonrodent toxicity studies: a review of regulatory guidelines and a survey of current practices. *Toxicol Pathol.* 2007;35(5):742-750.
19. Nemeth E. Iron regulation and erythropoiesis. *Curr Opin Hematol.* 2008;15(3):169-175.
20. Fabriek BO, Dijkstra CD, van den Berg TK. The macrophage scavenger receptor CD163. *Immunobiology.* 2005;210(2):153-160.
21. Nath KA. Heme oxygenase-1: a provenance for cytoprotective pathways in the kidney and other tissues. *Kidney Int.* 2006;70(3):432-443.
22. Tracz MJ, Juncos JP, Croatt AJ, et al. Deficiency of heme oxygenase-1 impairs renal hemodynamics and exaggerates systemic inflammatory responses to renal ischemia. *Kidney Int.* 2007;72(9):1073-1080.
23. Marro S, Chiabrando D, Messana E, et al. Heme controls ferroportin1 (FPN1) transcription involving Bach1, Nrf2 and a MARE/ARE sequence motif at position −7007 of the FPN1 promoter. *Haematologica.* 2010;95(8):1261-1268.
24. Vinchi F, Gastaldi S, Silengo L, Altruda F, Tolosano E. Hemopexin prevents endothelial damage and liver congestion in a mouse model of heme overload. *Am J Pathol.* 2008;173(1):289-299.
25. Hvidberg V, Maniecki MB, Jacobsen C, Hojrup P, Moller HJ, Moestrup SK. Identification of the receptor scavenging hemopexin-heme complexes. *Blood.* 2005;106(7):2572-2579.
26. Smith A, Morgan WT. Hemopexin-mediated heme transport to the liver: evidence for a heme-binding protein in liver plasma membranes. *J Biol Chem.* 1985;260(14):8325-8329.
27. Smith A, Morgan WT. Transport of heme by hemopexin to the liver: evidence for receptor-mediated uptake. *Biochem Biophys Res Commun.* 1978;84(1):151-157.
28. Smith A, Morgan WT. Haem transport to the liver by haemopexin: receptor-mediated uptake with recycling of the protein. *Biochem J.* 1979;182(1):47-54.
29. Gburek J, Verroust PJ, Willnow TE, et al. Megalin and cubilin are endocytic receptors involved in renal clearance of hemoglobin. *J Am Soc Nephrol.* 2002;13(2):423-430.
30. Christensen EI, Birn H. Megalin and cubilin: multifunctional endocytic receptors. *Nat Rev Mol Cell Biol.* 2002;3(4):256-266.
31. Rae F, Woods K, Sasmono T, et al. Characterisation and trophic functions of murine embryonic macrophages based upon the use of a Csf1r-EGFP transgene reporter. *Dev Biol.* 2007;308(1):232-246.
32. Pittock ST, Norby SM, Grande JP, et al. MCP-1 is up-regulated in unstressed and stressed HO-1 knockout mice: pathophysiologic correlates. *Kidney Int.* 2005;68(2):611-622.
33. Eskew JD, Vanacore RM, Sung L, Morales PJ, Smith A. Cellular protection mechanisms against extracellular heme: heme-hemopexin, but not free heme, activates the N-terminal c-jun kinase. *J Biol Chem.* 1999;274(2):638-648.
34. Jemnitz K, Heredi-Szabo K, Janossy J, Ioja E, Vereczkey L, Krajcsi P. ABCC2/Abcc2: a multispecific transporter with dominant excretory functions. *Drug Metab Rev.* 2010;42(3):402-436.
35. Kondo H, Saito K, Grasso JP, Aisen P. Iron metabolism in the erythrophagocytosing Kupffer cell. *Hepatology.* 1988;8(1):32-38.
36. Buehler PW, D'Agnillo F, Hoffman V, Alayash AI. Effects of endogenous ascorbate on oxidation, oxygenation, and toxicokinetics of cell-free modified hemoglobin after exchange transfusion in rat and guinea pig. *J Pharmacol Exp Ther.* 2007;323(1):49-60.
37. Kartikasari AE, Wagener FA, Yachie A, Wiegerinck ET, Kemna EH, Winkels DW. Hepcidin suppression and defective iron recycling account for dysregulation of iron homeostasis in heme oxygenase-1 deficiency. *J Cell Mol Med.* 2009;13(9B):3091-3102.

Downloaded from http://ashpublications.net/blood/article-pdf/116/26/6054/1491311/zh805210006054.pdf by guest on 08 June 2024